pISSN 1598-298X / eISSN 2384-0749
*J Vet Clin* 33(6) : 385-388 (2016)
http://dx.doi.org/10.17555/jvc.2016.12.33.6.385

Journal of Veterinary Clinics
www.ksvc.or.kr

# 3D-printing Bone Model for Surgical Planning of Corrective Osteotomy for Treatment of Medial Patellar Luxation in a Dog

**Bumsoo Jeong†, Jaemin Jung†, Jiyoung Park, Seong Mok Jeong and Haebeom Lee[1]**

*College of Veterinary Medicine·Research Institute of Veterinary Medicine, Chungnam National University, Daejeon 305-764, Korea*

(Received: June 13, 2016 / Accepted: August 16, 2016)

**Abstract :** A 2-year-old, castrated male Chihuahua dog was referred for revision surgery for reluxation of the patella following surgery for medial patellar luxation (MPL) of the left stifle joint. On general inspection, the patient showed bilateral hindlimb weight-bearing lameness. On physical examination, bilateral non-reducible MPL was detected through palpation. Radiographs revealed bone deformities of both hindlimbs. Computed tomography (CT) was applied for a three-dimensional (3D) printing bone model to establish an accurate surgical plan. The bone plate was pre-contoured over the 3D-printing bone model after execution of corrective osteotomy and sterilized prior to use in surgery. Corrective osteotomy was performed through a staged, bilateral procedure. The patient showed improvement of limb function following surgery without reluxation of the patella. The use of 3D-printing bone model for accurate surgical planning of corrective osteotomy appears to be effective in increasing the accuracy of surgery. That may lead to successful surgical outcomes.

***Key words*** **:** medial patellar luxation, bone deformity, corrective osteotomy, surgical plan, 3D-printing bone model.

## Introduction

Medial patellar luxation (MPL) is one of the most common orthopedic diseases causing hindlimb lameness in dogs (13,16,18). Malalignment of the quadriceps mechanism may be the major cause of the condition (13). Therefore, appropriate realignment of the quadriceps mechanism is essential to have a successful surgical outcome for MPL.

For realignment of the quadriceps mechanism, surgical treatments for MPL such as trochlear block or wedge recession and tibial tuberosity transposition have been performed (1,13,17,19). In general, the surgical outcome of MPL with surgical treatments varies with the degree of luxation of the patella. Grade 2 and 3 MPL are considered to have a good outcome for treatment, whereas grade 4 MPL carries a poor outcome (4,9,14,19,21). Especially, surgical treatment for grade 4 MPL with bone deformity is very challenging (22).

Femoral corrective osteotomy has been recently reported as the surgical treatment for MPL with deformity of the distal femur (12). Corrective osteotomy combined with conventional surgical treatments can help to reestablish appropriate alignment of the quadriceps mechanism in a patient having grade 4 MPL with bone deformity. The surgical correction of MPL using corrective osteotomy has been reported to have a good surgical outcome (12,15). However, it has been demonstrated that inappropriate correction of femoral or tibial deformities can be a cause of reluxation of the patella. Therefore, it is important to accurately evaluate bone deformities, make an accurate surgical plan and perform surgery accurately (8).

Radiography has difficulties in the accurate evaluation of bone deformity, in that it provides only two-dimensional data and has difficulty in obtaining an ideal positioning (3,10). As a solution for these limitations, corrective osteotomy using a 3D-printing bone model has been shown to produce a good surgical outcome for the correction of bone deformities in human medicine. However, report of corrective osteotomy using a 3D-printing bone model is rare in veterinary medicine.

The purpose of this case report is to describe the surgical planning, the surgical technique and the clinical outcome of corrective osteotomy using a 3D-printing bone model in a patient having grade 4 MPL with severe bone deformities of the distal femur and the proximal tibia.

## Case

A 2-year-old, 2.85 kg, castrated male Chihuahua dog was presented for revision surgery for reluxation of the patella following surgery for MPL of the left stifle joint. On general inspection, the patient showed score 4 bilateral hindlimb weight-bearing lameness (9). Physical examination revealed pain and grade 4 MPL in the bilateral stifle joint. Palpation of the hindlimb allowed for appreciation of the deformity of the femur and tibia. Radiographic examination of both hindlimbs revealed varus deformity of the distal femur and valgus deformity of the proximal tibia in both hindlimbs (Fig 1A).

For the 3D-printing bone model, computed tomography (CT) was performed with 130 kVp, 150 mA, 1 mm slice thick-

†These authors contribute equally to this work
[1]Corresponding author.
E-mail : seatiger76@cnu.ac.kr

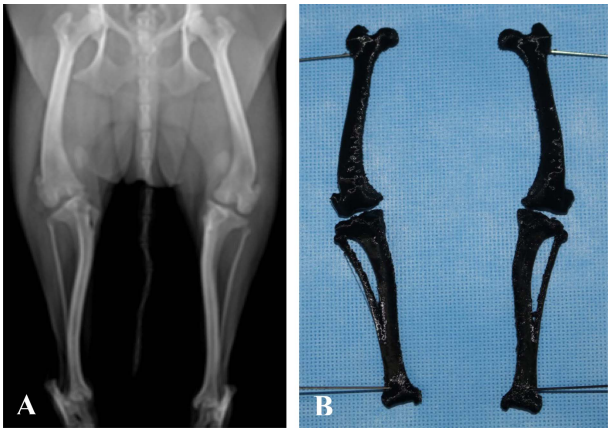


**Fig 1.** Preoperative ventrodorsal radiograph of both hindlimbs (A). 3D-printing bone model of both hindlimbs (B).

ness under general anesthesia using propofol (4 mg/kg IV, Provive®; Myungmoon Pharm, Korea) and isoflurane (Ifran®; Hana Pharm, Korea). The reconstructed CT data were used for rapid prototyping using a 3D printer. Bilateral femoral varus angle (FVA), tibial valgus angle (TVA) and anteversion angle were evaluated using the 3D-printing bone model (Fig 1B).

For accurate surgical planning, rehearsal surgery was performed using the 3D-printing bone model. The center of rotation of angulation (CORA) was found (Fig 2A). Each distance between the femoral condyle and the location of osteotomy and the correction angle of femoral torsion were measured (Fig 2B and C). Femoral closing wedge osteotomy was performed for a medial angular correction of 27° and an internal rotational correction of 15° for increasing anteversion angle (Fig 2D). The bone plate was pre-contoured over the 3D-printing bone model after the execution of corrective osteotomy and sterilized prior to use in surgery (Fig 2E). The identical method was used for the tibia.

Prior to surgery, premedication was carried out with glycopyrrolate (0.011 mg/kg SC, Morbinull®; Myungmoon Pharm, Korea), midazolam (0.2 mg/kg IV, Midazolam Inj®; Bukwang Pharm, Korea) and hydromorphone HCl (0.1 mg/kg IV, Dilid inj®; Hana Pharm, Korea). General anesthesia was induced

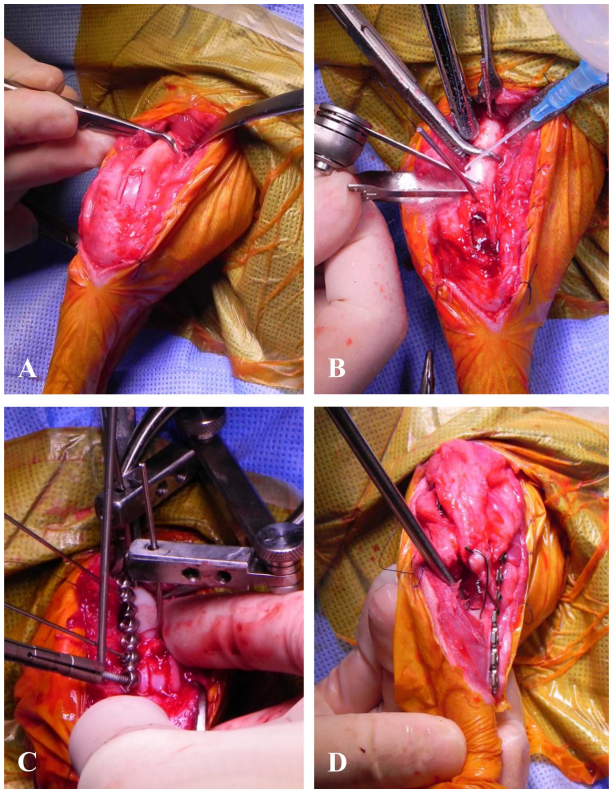


**Fig 3.** Intraoperative view. Lateral approach to the distal femur and trochlear block recession (A). Femoral wedge corrective osteotomy (B). Pre-contoured bone plate applied to the lateral aspect of the distal femur (C). Tibial wedge corrective osteotomy and tibial tuberosity transposition combined with tension band wiring (D).

with propofol (4 mg/kg IV, Provive®; Myungmoon Pharm, Korea) and was maintained with isoflurane (Ifran®; Hana Pharm, Korea) delivered in oxygen. Cefazolin (22 mg/kg IV q 2 hours, Cefazolin Inj®; Jong-Keundang, Korea) was administered prior to induction of anesthesia. The patient underwent epidural anesthesia with 0.5% bupivacaine (2 mg/kg, Bupivacaine HCL 0.5%®; Myungmoon Pharm, Korea). Intraoperative analgesia was maintained with remifentanil

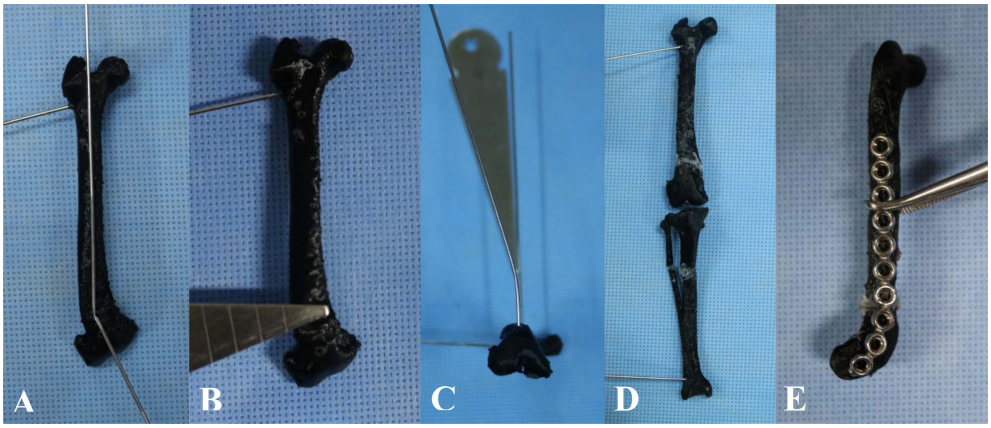


**Fig 2.** The center of rotation of angulation (CORA) visualized by Kirschner wires (A). Location of femoral wedge osteotomy (B). The distal TPLO jig pin that was bent laterally 15° (C). 3D-printing bone model following corrective osteotomy (D). The bone plate was pre-contoured over the postoperative 3D-printing bone model (E).

**Table 1.** Preoperative and postoperative measurement values for bone deformities of both hindlimbs

| | Preoperative | Postoperative | Reference |
|---|---|---|---|
| Right hindlimb | | | |
| FVA | 27° | 4° | < 5° |
| TVA | 24° | 7° | 5 ± 3° |
| Anteversion angle | 0°-1° | 16° | 15°-30° |
| Left hindlimb | | | |
| FVA | 22° | 3° | < 5° |
| TVA | 20° | 5° | 5° ± 3° |
| Anteversion angle | 0°-1° | 15° | 15°-30° |

FVA, Femoral varus angle; TVA, tibial valgus angle.

**Fig 4.** Postoperative ventrodorsal radiograph of both hindlimbs with appropriate limb alignment and bone healing at osteotomy sites.

HCl (0.1~0.6 μg/kg IV CRI, Ultiva®; GSK, UK).

The patient was positioned with dorsal recumbency and was prepared for aseptic surgery. A lateral approach was executed to the right distal femur and stifle joint and trochlear block recession was performed (Fig 3A). Then, the TPLO jig pins were placed cranio-caudally at the proximal and distal part of the osteotomy. The proximal jig pin was perpendicular to the proximal femoral sagittal axis and the distal jig pin was parallel to the articular surface of the stifle joint. Femoral closing wedge osteotomy with oscillating saw was performed (Fig 3B). For the correction of torsion, the distal fragment was rotated internally 15° using the distal jig pin. The proximal and distal fragments were reduced and the pre-contoured bone plate was applied to the lateral aspect of the distal femur (Fig 3C).

A medial approach was executed on the right proximal tibia and tibial closing wedge osteotomy was performed with an oscillating saw and two Kirschner wires as with the femur (Fig 3D). The pre-contoured bone plate was applied to the medial aspect of the proximal tibia (Fig 3D). Then, tibial tuberosity transposition and tension band wiring were performed after reevaluating patellar tracking and limb alignment (Fig 3D). Imbrication and releasing were also performed. The operative field was copiously lavaged and surgical incision was closed in layers.

Postoperative radiography revealed appropriate limb alignment and implant positioning. The FVA, TVA, and anteversion angle were evaluated with radiography and fluoroscopy (Table 1). Exercise restriction and gentle passive range of motion were performed on the patient for 6 weeks. Postoperative analgesia was maintained with a fentanyl patch (Matriphen patch 12 μg/hour; Daewoong Pharm, Korea) for 3 days following surgery. The patient was discharged with carprofen (2.2 mg/kg PO, two times daily, Rimadyl®; ZOETIS, Korea) and cephalexin (22 mg/kg PO, two times daily, Phalexin®; Dongwha Pharm, Korea) for 2 weeks.

On physical and radiographic examination at postoperative 5 weeks, there were no complications associated with the femoral and tibial osteotomy combined with conventional surgical treatments for MPL. Rehabilitation including passive range of motion, neuromuscular electrical stimulation, swimming and underwater treadmill was performed two times weekly. Three months postoperatively, the clinical function of the right hindlimb was significantly improved and almost normal.

Then, corrective osteotomy of the left hindlimb combined with conventional surgical treatments was performed identically. Postoperative radiographs revealed appropriate limb alignment and implant positioning in common with the right hindlimb. Six weeks postoperatively, the clinical function of the left hindlimb was improved.

At 1 year after surgery, the patient had recovered well and had a good functional outcome without lameness associated with activity. Radiographs showed satisfactory limb alignment and bone healing (Fig 4). The patient exhibited no luxation of the patella or complications.

## Discussion

The surgical correction of MPL with bone deformity is challenging (19). It is difficult to reestablish an appropriate alignment of the quadriceps mechanism using conventional surgical treatments.

In this case report, corrective osteotomy was performed for a patient having grade 4 MPL with severe bone deformities. The patient showed significantly improved limb function without postoperative reluxation of the patella.

For a successful corrective osteotomy, it is important to understand and evaluate the bone deformity accurately. However, accurate evaluation of bone deformity is hard to obtain by radiography (8). Radiography has several limitations: it provides only two-dimensional data for three-dimensional bone morphology, it is difficult to obtain ideal positioning for an accurate radiographic view and the surgeon has to reinterpret the results of radiography three-dimensionally. CT has been reported to solve these limitations of radiography for corrective osteotomy (2,6,17). In this case, a 3D-printing bone model created using CT data was used for corrective osteotomy. The 3D-printing bone model aided in evaluating

bone deformity accurately, made it possible to make an accurate surgical plan at a 1:1 ratio with the real bone of the patient and allowed the surgeon to confirm the planned surgical procedure through a rehearsal surgery. Furthermore, the rehearsal surgery using the 3D-printing bone model raised familiarity with the surgical procedure and the confidence of the surgeon and made the pre-contouring of bone plates possible. In human medicine, previous case studies have reported that using a 3D-printing bone model allowed for a successful clinical outcome by increasing surgical accuracy, decreasing surgical and therefore anesthetic time and aiding understanding both by the clinicians involved and by the client (5,11,20). Patients who need a challenging corrective osteotomy for bone deformity are definitely expected to benefit from the use of 3D-printing bone modeling (7).

3D-printing bone modeling using CT is disadvantageous in that it may be expensive. However, considering the extra cost from many radiographs and the inaccurate surgical plan and surgical failure that requires prolonged hospitalization or revision surgery, it may be rather economical.

## Conclusion

In this case report, corrective osteotomy was performed for the treatment of grade 4 MPL with severe bone deformity. 3D-printing bone modeling using CT can be very useful to make an accurate surgical plan and perform corrective osteotomy successfully.

## Acknowledgement

This work was supported by Basic Science Research Program through the National Research Foundation of Korea funded by the Ministry of Education, Science and Technology (NRF-2015R1D1A1A01056945).

## References

1. Arthurs GI, Langley-Hobbs SJ. Complications associated with corrective surgery for patellar luxation in 109 dogs. Vet Surg 2006; 35: 559-566.
2. Barnes DM, Anderson AA, Frost C, Barnes J. Repeatability and reproducibility of measurements of femoral and tibial alignment using computed tomography multiplanar reconstructions. Vet Surg 2015; 44: 85-93.
3. Crosse KR. Worth AJ. Computer-assisted surgical correction of an antebrachial deformity in a dog. Vet Comp Orthop Traumatol 2010; 23: 354-361.
4. DeAngelis M. Patellar luxation in dogs. Vet Clin North Am Small Anim Pract 1971; 1: 403-415.
5. D'Urso PS, Barker TM, Earwaker WJ, Bruce LJ, Atkinson RL, Lanigan MW, Arvier JF, Effeney DJ. Stereolithographic biomodelling in cranio-maxillofacial surgery: a prospective trial. J Craniomaxillofac Surg 1999; 27: 30-37.
6. Fitzpatrick CL, Krotscheck U, Thompson MS, Todhunter RJ, Zhang Z. Evaluation of tibial torsion in Yorkshire Terriers with and without medial patellar luxation. Vet Surg 2012; 41: 966-972.
7. Harrysson OLA, Cormier DR, Marcellin-Little DJ, Jajal K. Rapid prototyping for treatment of canine limb deformities. Rapid Prototyp J 2003; 9: 37-42.
8. Meggiolaro S. Isola M. Morgante M. Comparison of 3-dimensional model and standard radiographic evaluation of femoral and tibial angles in the dog. Arch Vet Ital 2009; 29: 38-63.
9. Monk ML, Preston CA, Mcgowan CM. Effects of early intensive postoperative physiotherapy on limb function after tibial plateau leveling osteotomy in dogs with deficiency of the cranial cruciate ligament. Am J Vet Res 2006; 67: 529-536.
10. Motari AC, Rahal SC, Vulcano LC, Silva VC, Volpi RS. Use of radiographic measurements in the evaluation of dogs with medial patellar luxation. Can Vet J 2009; 50: 1064-1068.
11. Murphy SB, Kijewski PK, Simon SR, Chandler HP, Griffin PP, Reilly DT, Penenberg BL, Landy MM. Computer-aided simulation, analysis, and design in orthopedic surgery. Orthop Clin North Am 1986; 17: 637-649.
12. Persuki AM, Kowaleski MP, Pozzi A, Dyce J, Johnson KA. Treatment of medial patellar luxation and distal femoral varus by femoral wedge osteotomy in dogs: 30 cases (2000-2005). Proceedings of the 2nd World Veterinary Orthopaedic Congress and 33rd Annual Veterinary Orthopedic Handbook of Small Animal Orthopedics and Fracture Repair Society Meeting. Keystone: Veterinary Orthopedic Society, 2006: 240.
13. Piermattei DL, Flo GL, DeCamp CE. The stifle joint. In: Handbook of Small Animal Orthopedics and Fracture Repair. 4th ed. Philadelphia: Saunders. 2006: 562-582.
14. Remedios AM, Basher AW, Runyon CL, Fries CL. Medial patellar luxation in 16 large dogs a retrospective study. Vet Surg 1992; 21: 5-9.
15. Roch SP, Gemmill TJ. Treatment of medial patellar luxation by femoral closing wedge ostectomy using a distal femoral plate in four dogs. J Small Anim Pract 2008; 49: 152-158.
16. Schulz KS. Diseases of the Joints. In: Small Animal Surgery. 4th ed. St. Louis: Mosby Elsevier. 2013: 1215-1374.
17. Towle HA, Griffon DJ, Thomas MW, Siegel AM, Dunning D, Johnson A. Pre- and postoperative radiographic and computed tomographic evaluation of dogs with medial patellar luxation. Vet Surg 2005; 34: 265-272.
18. Vasseur PB. Stifle joint. In: Textbook of Small Animal Surgery. 3rd ed. Philadelphia: Saunders. 2003: 2090-2132.
19. Wangdee C, Theyse LF, Techakumphu M. Evaluation of surgical treatment of medial patellar luxation in Pomeranian dogs. Vet Comp Orthop Traumatol 2013; 26: 435-439.
20. Webb PP. A review of rapid prototyping (RP) techniques in the medical and biomedical sector. J Med Eng Technol 2000; 24: 149-153.
21. Willauer CC, Vasseur PB. Clinical results of surgical correction of medial luxation of the patella in dogs. Vet Surg 1987; 16: 31-36.
22. Yasukawa S, Edamura K, Tanegashima K, Seki M, Teshima K, Asano K, Nakayama T, Hayashi K. Evaluation of bone deformities of the femur, tibia, and patella in Toy Poodles with medial patellar luxation using computed tomography. Vet Comp Orthop Traumatol 2016; 29: 29-38.